Effective Parameters Optimization of a Small Scale Gorlov Wind Turbine, Using CFD Method

Akhlagi, Mohammad [*+]***; Ghafoorian, Farzad***

Turbomachinery Research Laboratory, Department of Energy Conversion, School of Mechanical Engineering, Iran University of Science and Technology, Tehran, I.R. IRAN

Mehrpooya, Mehdi [*+]

Hydrogen and fuel cell laboratory, Faculty of New Sciences and Technologies, University of Tehran, Tehran, I.R. IRAN

Sharifi Rizi, Mohsen

Department of Energy Conversion, School of Mechanical Engineering, Iran University of Science and Technology, Tehran, I.R. IRAN

ABSTRACT: *In the present study, a Gorlov Vertical Axis Wind Turbine (VAWT) in small dimensions was numerically simulated using the Computational Fluid Dynamics (CFD) method. The purpose of this study is to investigate the effect of design and operational parameters on the Gorlov VAWT performance. In order to evaluate the efficiency of this turbine, two parameters of power and torque coefficients are calculated, and their values are compared in the different tip speed ratios (TSR). This paper investigates effective parameters namely inlet wind velocity, blade chord length, helical angle, aspect ratio, and blade airfoil profile. The results show that the turbine with V=15(m/s), c =0.25(m), ψ =30(deg), φ= 2.3 increased maximum C_p by 75%, 273%, 30% and 250%, respectively. In order to find optimal conditions to achieve a higher value of C_p, the Kriging optimization method is provided. The results of C_p show that the highest efficiency of Gorlov VAWT is related to an inlet wind velocity of 15 (m/s), the aspect ratio of 2.3, helical angle of 30 degrees, chord length of 0.25 (m), and NACA0018 airfoil profile at TSR of 1.8. Also, sensitivity analysis indicates that blade chord length and helical angle have more effect on mentioned VAWT performance. The C_p and C_m in the mentioned conditions are high enough thus it helps self-starting capability.*

KEYWORDS: *vertical axis wind turbine; Gorlov wind turbine; power coefficient; torque coefficient; CFD simulation; tip speed ratio.*

INTRODUCTION

Rising concerns about global warming and pollution of the environment have boosted interest in renewable energy. Renewable fuel sources such as wind energy, solar energy, hydropower, geothermal energy, and biomass are

*To whom correspondence should be addressed.

+ *E-mail: mohammad.akhlaghi@iust.ac.ir , mehrpoya@ut.ac.ir*

1021-9986/2023/7/2286-2304 19/$/6.09

good alternatives to fossil fuels. In the meantime, wind energy in some areas can be the appropriate alternative energy and also, in some regions hybrid systems can provide claen energy[1, 2]. Significant growth in wind energy in 2009 became a world record. This amount increased from 37 GWh to 158 GWh[3]. Today, wind turbines are coupled with solar panels and fuel cells and have been popular with the public by producing electricity with minimal emissions and optimal efficiency[4]. Wind turbines are classified into different perspectives. One of the most common classifications of wind turbines is based on the type of rotating shaft. This view divides wind turbines into two categories: Vertical Axis Wind Turbines (VAWT) and Horizontal Axis Wind Turbines (HAWT) [1]. Today, most commercial wind turbines belong to HAWTs. The advantages of these types of wind turbines include high efficiency and high extractable power[5]. One of the disadvantages of HAWTs is their very complex control systems which are very expensive and their technical analysis requires complex calculations[6]. On the opposite side, VAWTs have many advantages; they are not sensitive to wind stream direction; therefore, they have a simpler structure and do not require a yaw system. Because the generator, gearbox, and other major components of the turbine can be mounted on the ground, the design and construction of the structure become very simple, thus reducing the cost of the turbine[7]. The maximum practical height is limited because the wind turbine shaft is only supported at one end at ground level. Due to their lower efficiency, only a small percentage of wind turbines are VAWTs. However, they can potentially develop[8]. Several types of VAWTs are utilized in the industry, including Darrieus, Savonius, and Gorlov turbines, to name but a few. The Darrieus wind turbine, known as the egg stirrer, was invented in 1931 by George Darrieus. The Darrieus consider as a high-speed, low-torque machine designed to generate power. Darrieus turbines typically require starting torque to start rotating, and it is considered one of the disadvantages of this type of wind turbine. This turbine operates with the help of lift force [9]. Savonius turbine is a VAWT that Sigurd Savonius invented in 1925, which works based on drag forceb[10]. This turbine is generally composed of two buckets, concave and convex. The turbine's operation is such that the wind applies a force in its direction to the turbine blades; the reason for the rotation of the rotor is that the post-wind force in the concave part is more than the convex part. Due to its high torque, it is suitable for applications such as pumping water from wells[11]. Another advantage of this type of rotor is that they do not need initial torque[12]. Many design parameters, including the arc angle of the buckets, overlap ratio, buckets spacing and shape factor affect the performance of this turbine[13]. One of the common studies performed is the construction of hybrid vertical axis wind turbines. In this method, a Savonius turbine is combined with a Darrieus turbine or even a Gorlov and a spiral to increase the overall efficiency and by installing the Savonius turbine the initial torque problem is solved. This study has been done to optimize performance in medium-low wind regimes and result shows that combined turbine performance improved in low TSRs[14,15]. Another vertical axis wind turbine that is very popular today is the Gorlov vertical axis wind turbine, which works like a Darrieus turbine with lift force[16]. Gorlov helical turbine was designed in 1995 by Russian researcher Alexander Gorlov to reduce the periodically unsteady torques compared to the Darrieus type and increase turbine efficiency[17]. This power generator was first used as a cross-flow water turbine and was used as a tidal turbine to extract hydropower from the tidal energy of water stream waves[18]. This cross-flow water turbine was also used as a water turbine in shallow running water and rivers. For example, in India's Mahatma Gandhi hydroelectric power plant, Gorlov water turbines were used to generate power[19]. The hydrodynamic performance of the Gorlov turbine as a water turbine was investigated numerically and experimentally in a water tunnel, and the power coefficient and torque coefficient were considered. The results showed good efficiency for this turbine[20]. In an numerical simulation nine Gorlov VAWTs with the height and diameter of 0.6(m) which was installed in shallow water as micro-hydropower system was examined and acceptable power was harvested[21]. The most important advantage of this turbine is that the unfavorable vibration is reduced compared to H-rotor Darrieus VAWT, and also self-starting ability improved remarkably[19]. Also, a configuration similar to the structure of the Gorlov turbine in the path of water pipes was used. The name of this cross-flow turbine that worked with a fast flow of water inside the pipe was Lucid[22]. A comparison between hydrodynamic and geometric parameters of a Gorlov helical hydrokinetic turbine and a Lucid spherical turbine

has been investigated by adopting experimental and numerical approaches; the result indicated that the Gorlov turbine was more efficient for marine applications [23]. The 3D investigation was performed to determine the difference between the straight and helical blade accurately, and the result proved that in low TSRs, the helical turbine had better behavior [24].Different solving methods, namely 2D LES, 2D, and 3D U-RANS, were compared, and the 3D-URANS approach was best fitted to the experiment results [25]. To solve the starting problem in low TSRs, optimal blade weight was considered and manufactured by a 3D printer [26]. For this purpose, in the construction of the Gorlov turbine, parameters such as. Chord length, blade height, helix angle, aspect ratio, and airfoil profile were considered[27]. A smooth rotor surface significantly enhanced turbine efficiency and obtaining pitch angle at the starting point improved performance [28]. Experimental tests require special facilities and sometimes high costs, so researchers study the parameters of various wind turbines using methods and numerical modeling, including CFD 2-D or 3-D solutions and DMST and MST solutions[29]. For example, the DMST solution was performed on a Darrieus turbine called Sandia, which was 17 meters height, and the extractable power of this turbine at different wind velocities was investigated [30]. DMST solution was also performed on a Gorlov turbine, and the effect of different geometrical parameters such as helical angle and aspect ratio on power and torque coefficients was investigated [17]. Also, using the same solution, a parametric study was performed on a Darrieus and Gorolv turbine, and their efficiency and performance were compared [31]. On the other hand, with experimental studies in different wind tunnels, it was found that turbulent and wake flows behind the turbine significantly affect the efficiency and performance of wind turbines [32]. CFD-based solutions and LES-based codes have also been shown to model turbulent and wake flow behind the turbine, providing more accurate answers for efficiency and parametric studies[33, 34]. The effect of turbulent flow and turbulence intensity is so important and effective that different turbulence models can dramatically effective; the results indicate that k-epsilon and k-omega models are suitable methods [35]. An experimental study has been performed to show the effects of the wake flow regime behind each wind turbine on the array of wind turbines. It has been stated that the distance between wind turbines in wind farms should be a certain value[36]. In a numerical simulation, two VAWT rotors with a certain distance and different rotational directions were investigated. The results showed that their rotational direction (co-rotating and counter-rotating) and the wake flow created in the downstream section of them significantly affect the C_p values [37]. Also, to show the importance of wind velocity in the region on the performance of wind turbines, a VAWT was evaluated in unsteady wind flow in the wind tunnel, and its performance was increased by increasing wind velocity at any TSRs[38]. About wind tunnel test, by installing a diffuser in the opening of the wind tunnel, the performance of the wind turbine was improved, by directing wind flow additionally by changing the values of the angles and length of the diffuser, an optimal diffuser was provided for installation in the exit opening of the wind tunnel [39]. Also dynamic stall can effect VAWTs aerodynamic performance, in a numerical study by delaying dynamic stall, exergy destruction decrease, and subsequently, turbine efficiency improved [40] . Different chord length and helical angle values were obtained and C_p of optimal geometry was 13.7% greater than base geometry [41]. Index of revolution which is the ratio between height and pitch of helical blades has been studied and the results show that index of revolution of 0.25 gave highest generated power [42]. Increasing number of blade from two to three remarkably declined tourqe value at all TSRs, also increasing number of blade from three to four, further reduced tourqe value at low TSRs with constant solidity [43]. The results showed that in TSR less than four, turbines equipped with blades with larger chords give higher power coefficient values however, in high TSRs the opposite result is achieved [44]. Also, in a numerical study, the dynamic stall, which is caused by massive flow separation and the creation of unfavorable vortices on the turbine blade, has been reduced by optimizing the chord length size and tangential force [45]. Effect of aspect ratio and Reynolds number on the performance of a Darrieus VAWT was numerically studied and the values of power coefficient increased by raising mentioned values[46]. In another study, changes in the geometry and structure of the airfoil were examined and slotted airfoil was used to improve performance of a H-type Darrieus [47]. Also, by making another change in the geometry of the airfoil and considering a dimple at the lower edge of the airfoil,

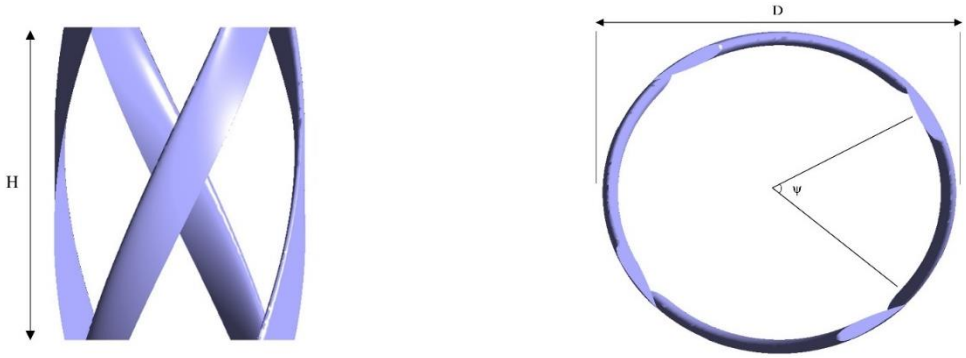

Fig.1: Schematic of the 4 blade Gorlov VAWT studied

the performance of the Darrieus wind turbine was improved[48]. Increasing solidity in Darriues VAWT by number of blade to 5 showed higher tourqe and power values in low TSRs however 2 blade turbine had better performance at high TSRs [49]. The effect of airfoil profile on the performance and efficiency of vertical axis wind turbine for NACA0012 and NACA4415 airfoils was also evaluated to determine the best type of airfoil for designing a VAWT. It should be noted that a wide range of airfoil types for turbine blades can be considered [50]. For information and general specifications of airfoils, refer to X-foil commercial software which contain useful parameters such as lift coefficient and drag coefficient[51]. In helical VAWTs such as Gorlov wind turbine the effect of the of the helical angle on the performance can be investigated [52]. Many studies have worked on optimizing turbines, the main purpose of which has been to find an optimal geometry for a turbine. One of the common methods has been to use genetic algorithms [53]. To optimize airfoils and hydrofoils, a combination of genetic algorithm and hierarchical fair competition model can be used and their performance can be evaluated with conventional airfoils such as NACA0012 [54]. Also the influence of artificial intelligence on different configurations of Savonius turbine blades has been investigated and the best twist angle and shape factor for this model have been presented through artificial intelligence[55]. Another method that has been used to optimize the performance of wind turbines has been the Taguchi method in association with modified additive model. This method has been used with upper and lower deflector to find propper instaltion[56]. Another method used to optimize VAWTs is the Particle Swarm Optimization (PSO) method, which optimizes according to a certain known model (Surrogate model). The certain known model is obtained using the Kriging method, which can show the optimized C_p in different operating conditions[57, 58]. Another optimization method is Design Of Experiment (DOE) and the purpose of the DOE is to select each design parameter to describe the shape design space well. Considering the rather negligible number of control points, a factorial method is suitable in this approach[59]. In fact for optimization with DOE methods, there are optimization techniques including Mixture design, Taguchi, and Response Surface Methodology, the first one is for formulation, the second one is for process conditions, and the third one has simultaneous application for process and formulation changes[60]. However the RSM method has two techniques. One is Central Composite Design (CCD), which can simultaneously model and optimize 2 to 9 factors (independent variable) with a large number of responses (dependent variable). The other is Box-Behnken Design (BBD), which can model 3 to 7 factors with a large number of responses. (dependent variable) models and optimizes[61].

Regarding the literature mentioned above review, a 3D numerical study of the effect of various parameters such as wind velocity, blade chord, aspect ratio, helical angle and blade airfoil profile on the efficiency of the Gorlov VAWT, which is a lift-based turbine and its performance is better than a simple straight blade Darrieus VAWT, has been rarely investigated. The CFD analysis was conducted by finite volume commercial software, ANSYS CFX based on the U-RANS equation to evaluate the influential parameters. Finally, using the Kriging method, which is a reliable approach, the optimal geometry and operating condition was selected to aquire highest performance.

Table 1: Dimensions and specifications of the simulated turbine

	Quantity	Value
1	Number of blade	4
2	Profile of blade	NACA0018
3	Length of chord	0.1 (m)
4	Radius of rotor	0.21 (m)
5	Helical angle	70°
6	Height of blade	0.54 (m)
7	Wind velocity	9 (m/s)
8	Rotational speed	55-99 (rad/s)
9	Solidity	1.9
10	Swept area	0.23 (m^2)

Table 2: Dimensions of the domain or stator

	Quantity	Value
1	Length of stator	21(m)
2	Width of stator	3(m)
3	Height of stator	5(m)

THEORETICAL SECTION

Problem description and solution strategy

In the present study, for numerical simulation, a type of Gorlov vertical axis turbine is considered a prototype. This turbine consists of four helical blades, and its helical angle is assumed to be 70 degrees. In this analysis, the arms and shaft are not considered to have more concentration on the aerodynamic behavior of the blades and facilitate meshing and reduce the calculation time. The schematic of the studied Gorlov turbine is given in Fig.1.

Dimensions and characteristics of turbine and geometry are given in Table 1.

In this numerical simulation, a large rectangular cube is considered a computational domain called the stator. The dimensions of the comparative domain or stator are given in Table 2.

Fluid mechanics, aerodynamic, and turbulence flow equations

In CFD analysis, the Navier-Stokes equation simulates the flow around the Gorlov turbine rotor. In this section, Reynolds averaging is used, and the speed is divided into two terms, $\bar{u}$ and u' which are called the average term and the fluctuating term. Also, equations 3 and 4 represent the Unsteady Reynolds Average Navier Stokes (URANS)[29].

$$\overline{u} = \frac{1}{T}\int_T u(t)dt \text{[29]} \quad (1)$$

$$u' = u - \overline{u} \text{ [29]} \quad (2)$$

$$\frac{\partial \overline{u_i}}{\partial x_i} = 0 \text{ [29]} \quad (3)$$

$$\frac{\partial \overline{u_i}}{\partial t} + \overline{u_j}\frac{\partial u_i}{\partial x_j} = -\frac{1}{\rho}\frac{\partial \overline{p}}{\partial x_i} + \nu\frac{\partial^2 \overline{u_i}}{\partial^2 x_j^2} - \overline{u_j'\frac{\partial u_i'}{\partial x_j}} \text{ [29]} \quad (4)$$

Where u is the velocity of fluid flow (m/s) component, x is the direction (m) component, p is pressure (Pa), and ρ (kg/m^3) is the fluid density.

Turbulent flow equations are another fundamental governing equation that is very important and remarkably impacts CFD modeling and solving. Two turbulence equation models have been widely used over the years and have been accepted as a suitable compromise between accuracy and computational cost. These two models are called k-ε and k-ω. Both models use the Boussinesq assumption shown in Eq. (5) for Reynolds stresses [62].

$$\tau_{ij} = 2\mu_t\left(S_{ij} - \frac{1}{3}\frac{\partial u_k}{\partial x_k}\delta_{ij}\right) - \frac{2}{3}\rho k\delta_{ij} \text{ [62]} \quad (5)$$

$$S_{ij} = \frac{1}{2}\left(\frac{\partial u_i}{\partial x_j} + \frac{\partial u_j}{\partial x_i}\right) \text{[62]} \quad (6)$$

The k-ε model was used in this study. One of the advantages of using this model is the reduction of computational costs for modeling turbulent flows. Also, this approach is widely used for modeling the flow around turbomachines. Additionally, the k-ε equations for applications near wall regions are suitable [63]. Finally, this turbulence model has the capability of predicting boundary layer separation and capturing dynamic stall, which are important features to indicate Gorlov turbine's advantage over straight-blade turbines [45]. These models are based on transport equations for the turbulence kinetic energy, k, and its dissipation rate ε. The model uses the following transport equations:

$$\frac{Dk}{Dt} = \frac{1}{\rho}\frac{\partial}{\partial x_k}\left[\frac{\mu_t}{\sigma_k}\frac{\partial k}{\partial x_k}\right] + \frac{\mu_t}{\rho}\left(\frac{\partial U_i}{\partial x_k} + \frac{\partial U_k}{\partial x_i}\right)\frac{\partial U_i}{\partial x_k} - \varepsilon \text{ [62]} \quad (7)$$

$$\frac{D\varepsilon}{Dt} = \frac{1}{\rho}\frac{\partial}{\partial x_k}\left[\frac{\mu_t}{\sigma_\varepsilon}\frac{\partial \varepsilon}{\partial x_k}\right] + \frac{C_1\mu_t}{\rho}\frac{\varepsilon}{k}\left(\frac{\partial U_i}{\partial x_k} + \frac{\partial U_k}{\partial x_i}\right)\frac{\partial U_i}{\partial x_k} - C_2\frac{\varepsilon^2}{k} \text{[62]} \quad (8)$$

The turbulent viscosity is assumed from the below equation:

$$\mu_t = \rho C_\mu \frac{k^2}{\varepsilon} \text{ [62]} \quad (9)$$

Table 3: values and constants of the RNG k-ε model [35]

C_μ	$C_{\varepsilon 1}$	$C_{\varepsilon 2}$	σ_k	σ_ε
0.0845	1.42	1.68	0.7194	0.7194

The other parameters of the above equation are obtained from Table 3.

After understanding the equations related to turbulent flow modeling and U RANS, the governing equations of the Gorlov wind turbine model and the mathematical relations that can be used to study its performance and efficiency are considered. For vertical and horizontal axis wind turbines, the tip speed ratio is defined as the ratio between the rotation (ω) of the blade tip and the actual wind speed (V_w). The following mathematical relation is established for the tip speed ratio if the tip velocity is exactly equal to the wind velocity [29].

$$TSR = \frac{R \times \omega}{V_w} \text{ [29]} \quad (10)$$

Where *R(m)* is the radius of the turbine rotor, ω(rad/s) is the rotor angular velocity, and V_w(m/s) is the inlet wind velocity.

Another operating parameter is the overall torque of the turbine, which results from a complete rotation of the blade [29]. Two other important parameters for wind turbines are power coefficient (C_p) and torque coefficient (C_m), which are appropriate criteria for checking the turbine's efficiency.

$$C_p = \frac{P}{0.5 \times \rho \times A \times V_w^3} \text{ [64]} \quad (11)$$

$$C_m = \frac{T}{0.5 \times \rho \times A \times R \times V_w^2} \text{ [64]} \quad (12)$$

Where ρ (kg/m^3) wind densities, V_w (m/s) is wind speeds entering the turbine, T (N.m) is turbine torque, P (W) is the extractable power, and A (m^2) is the swept area. The swept area is calculated from the following equation[64].

$$A = D \times H \text{ [64]} \quad (13)$$

Where D(m) is rotor diameter and H(m) is turbine height.

The following mathematical relation is also assumed between the extractable power and the turbine torque. Equation 14 also shows the relation between the number of turbine rotations and the angular velocity[64].

$$P = T \times \omega \text{ [64]} \quad (14)$$

$$N = \frac{30 \times \omega}{\pi} \text{ [64]} \quad (15)$$

Where N(rpm) is the number of turbine rotation.

The aspect ratio that is considered for the design of vertical axis wind turbines is defined as a mathematical equation. This mathematical relation indicates that the aspect ratio depends on the height and radius of the turbine rotor.

$$\varphi = H/2R \text{[31]} \quad (16)$$

Another critical parameter in the design of wind turbines is called solidity. This quantity depends on the number of turbine blades, chord length, and radius. This quantity is defined as follows.

$$\sigma = nc/R \text{ [31]} \quad (17)$$

In this equation, n is the number of blades, and c(m) is the blade chord length.

Numerical modeling and simulation

Model design, meshing, and boundary condition

The geometries mentioned in Figs. 1 and 2 are coupled for numerical modeling. The turbine is inside a computing domain that can be the test section of a wind tunnel or an open region. The turbine and the computing domain have been grided. Meshing is done in ANSYS Meshing software. For generating mesh an unstructured grid was chosen for both rotor and stator. Also, the all triangles method was used for the rotor and stator domains. In order to more precise CFD results and to capture the effects of flow separation around the leading and trailing edges of blades, a suitable grid size and boundary layer mesh, which contains 8 layers with a growth factor of 1.1, were adopted. And as the k-epsilon turbulence model has some problems in flow behavior prediction around blades, the accurate boundary layer mesh prepare acceptable y+ value which helped to gain more accurate CFD results and flow behavior prediction around blades. The meshed geometry is then entered into the finite volume analysis software ANSYS CFX. At this stage, the boundary and initial conditions for analysis are defined. For the boundary conditions governing the problem, the front side of the rectangular cube is considered the system wind flow; thus, it is defined as the boundary condition of the velocity inlet and inlet velocity of 9(m/s) was considered as initial condition. Other sides of the rectangular cube are regarded

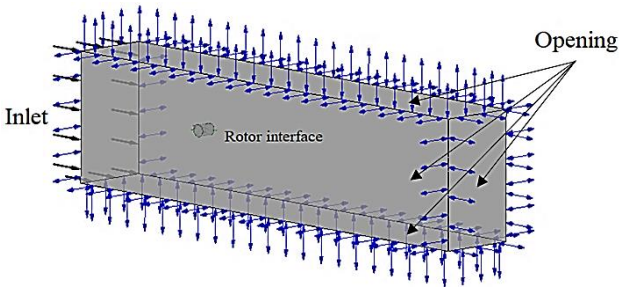

Fig.2: Rotor and Stator set with boundary conditions

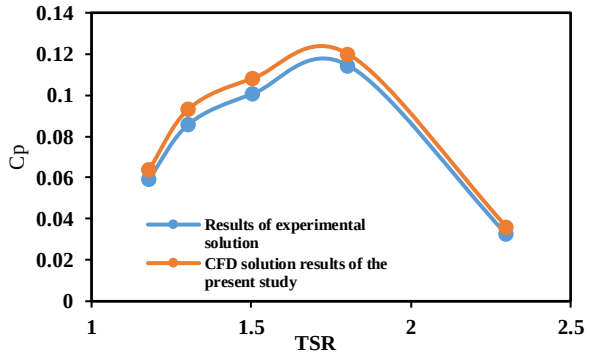

Fig.3: C_P values obtained with CFD solution compared with the results of the experimental study

as the opening condition in which air flows out, and because that is far from the turbine, and in these areas that are in direct contact with the free airflow, a pressure of 1 atmosphere is considered. Also, based on the inlet velocity value and the dimensions of the prototype, Reynolds number is 60000; therefore turbulent flow regime is adopted for this simulation. The interfaces were defined between rotor and stator. Fig.2 shows the rotor and stator assemblies. The black arrows are for the velocity inlet condition, and the blue arrows are for the opening condition.

Also, as the position of rotor changed in different time steps, in this 3D simulation transient approach has been adopted. The high resolution selected for advection scheme and second order backward Euler adopted for transient scheme with RMS convergence criteria for solver settings.

Validation and grid independence

After meshing and applying the boundary conditions, it is essential to validate the designed model and the numerical analysis with an experimental study that has already been done. For this purpose, an experimental study performed on a four-blade Gorlov turbine is selected. This

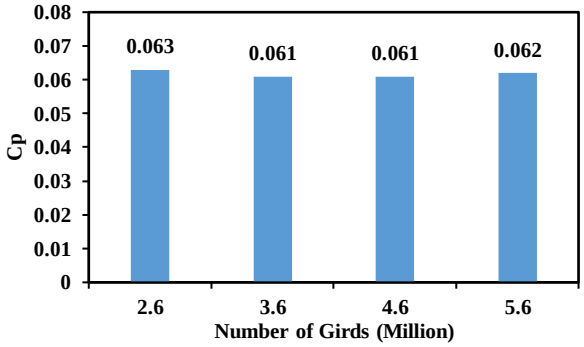

Fig.4: C_P values at the tip speed ratio of 1.17 in different grids

experimental test was performed inside a wind tunnel with an inlet velocity of 9 m/s, according to the considered TSRs and the inlet wind velocity in the study of Cheng et al. [25]. And considering equations 10 and 15, the value of angular velocity ω (rad /s) and the number of rotations N (rpm) were obtained. The software must give these values calculated for five different TSRs to enable the analysis and calculation of extractable power. By knowing the amount of wind turbine output power and using Equation 11, the amount of C_p can be calculated.

The number of rotations and the angular velocity were determined at five different TSRs. With the help of data extracted from software and numerical analysis performed on the turbine, the amount of power that can be extracted for each of these five modes is obtained by using mathematical equation 11, which was proposed to calculate the power coefficient; these critical coefficient values are calculated in each of the five modes and then compared with the results obtained from the experimental study. The comparison results for C_p is shown in Fig.3.

As shown by the results in Fig.3, the study results and numerical simulation show acceptable agreement with the experimental study and the maximum error value was evaluated about 5%, so the method of numerical analysis is considered reliable. Another essential step that has been taken for the validity and of the solution is the grid independence solution. For performing this study, the C_p values in different grid numbers are evaluated at an arbitrary angular velocity and TSR. The number of grids considered for the four different modes was 2.6, 3.6, 4.6, and 5.6 million, and the value of the C_p in the tip speed ratio of 1.17 and angular velocity 50 (rad/s) in these four modes was investigated. The results can be seen in Fig.4.

As shown from the diagram in Fig.4, the values obtained for C_p are not significantly different in four

different cases, so the numerical solution does not depend on the number of meshes. From this perspective, numerical simulation is acceptable.

RESULTS AND DISCUSSION

In this section, the results obtained from turbine simulation are analyzed. As mentioned, several parameters are effective in the performance and efficiency of wind turbines. Some of them are considered in this study and are analyzed numerically. The prevailing wind speed of the region, helical angle, the chord length, which is effective in the solidity of the turbine, and the aspect ratio depends on the changes in radius and height are examined.

Effect of prevailing wind speed

The performance and efficiency of wind turbines are highly dependent on the system's wind speed. And with different values of wind flow speed, turbine efficiency will also change. Therefore to show the effect of wind speed on turbine performance, the mentioned Gorlov wind turbine was evaluated under three different wind speeds of 9(m/s), 12(m/s), and 15(m/s). The value of TSR is considered constant, and the input wind speed is regarded as a variable in five different TSRs. Obviously, according to equation 10, the value of angular velocity and the number of turbine rotations will be changed due to the constant radius of the rotor and TSR. It is noteworthy that with increasing wind speed and paying attention to not changing the radius and TSR, the values of angular velocity and number of rotations increase significantly.

Such as the validation section was analyzed in CFX finite volume analytics software. After numerical simulation, the power and torque coefficient values in specific TSRs were calculated at inlet wind speeds of 12(m/s) and 15(m/s) and compared with the results related to the input wind speed of 9(m/s), which had been previously calculated. The results of comparative graphs related to the values of C_p and C_m at different wind speeds are presented in Figs. 5 and 6.

As can be seen from Figs. 5 and 6, as the input wind speed increases from 9 (m/s)to 12 (m/s) and then 15 (m/s), the values for C_p and C_m increase. It should be noted that the two parameters, C_p and C_m, indicate the efficiency and performance of wind turbines. On the other hand, both forms indicate that the values of C_p and C_m do not always increase with increasing TSR, or in other words, with the increasing number of rotations, and from a certain

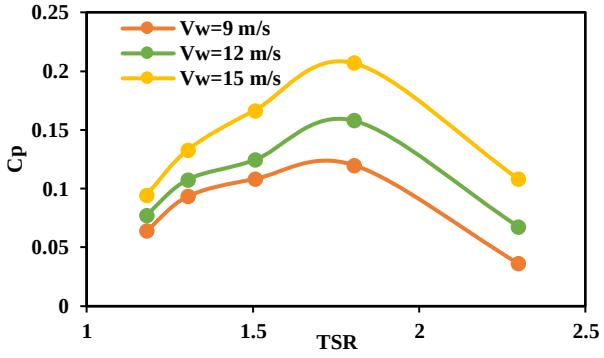

Fig.5: C_p Values at different wind speeds

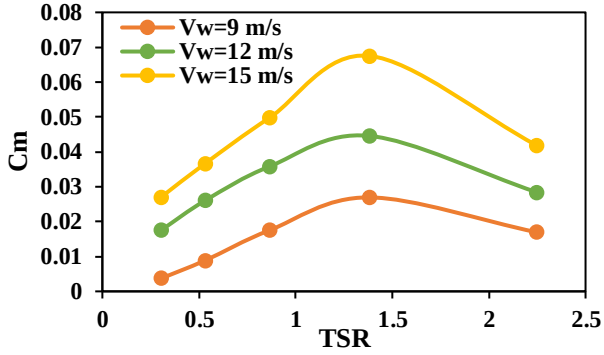

Fig.6: C_m Values at different wind speeds

onwards, the amount of efficiency decreases. As a result, to design a wind turbine, one design point is considered optimal operating conditions. In the above turbine and the existing operating conditions, the maximum efficiency of the turbine is obtained in TSR = 1.8. It is clear from Fig.5 that the maximum value of C_p,which is related to the wind speed of 15(m/s), is about 0.43, which was 75% higher than C_p value of V_w=9(m/s). Also, the highest value of C_m was related to wind speed 15(m/s), which occurred at TSR= 1.8, and its value was calculated to be equal to 0.068. Finally, considering the power coefficient values, it should be noted that the efficiency difference in low TSRs is not significantly Sensible. Still, with the increase of TSR, this difference in efficiency due to the rise in the inlet wind speed becomes more visible. To illustrate flow behavior around Gorlov VAWT contour plots are given in Fig.7.

Based on Figure7, as clearly seen by increasing inlet velocity, wake flow and low-velocity regime around blades decreased, and blade-to-blade interaction, which highly affects turbine power generation ability, reduced significantly. Additionally, the wake flow regime in the

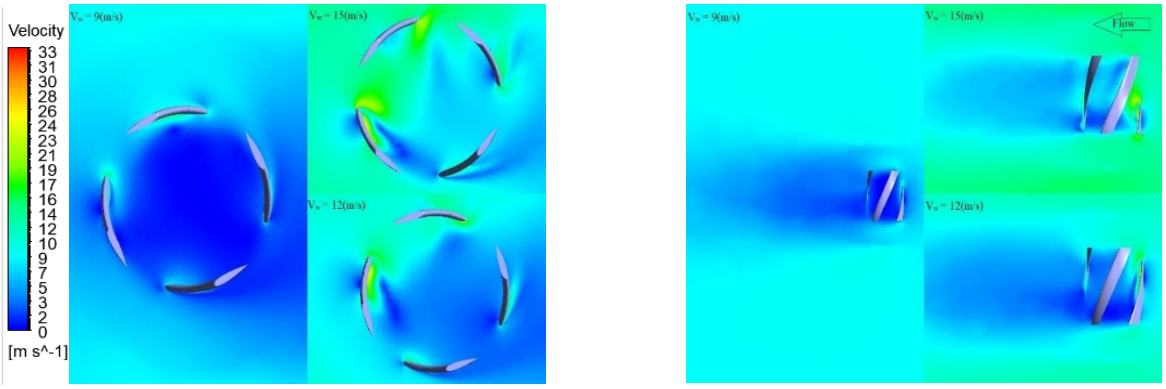

Fig.7: Velocity contour plots for different prevailing wind speed values

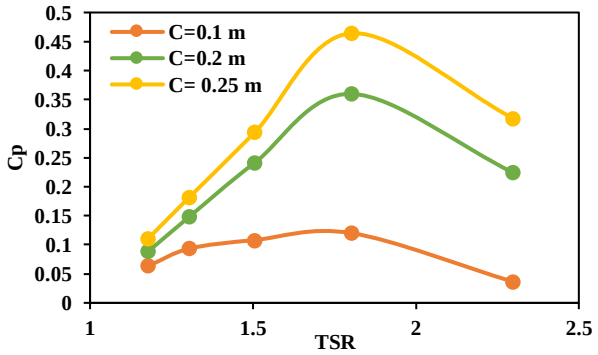

Fig.8: C_p values at different blade chords

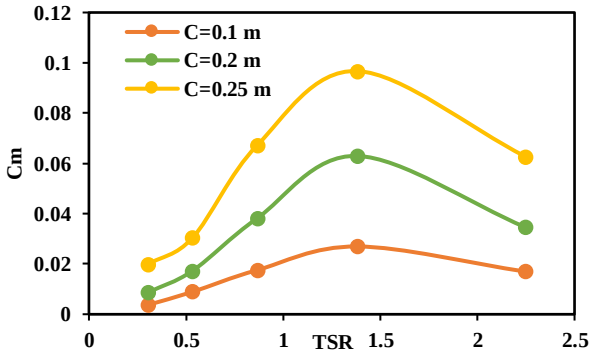

Fig.9: C_m Values at different blade chords

rotor downstream section declined significantly. Also, the turbine with lower inlet velocity caused the formation of flow stagnation at the upstream zone, resulting in the turbine's lack of access to a clear flow stream, and high-velocity regions near blade edges were more remarkable when the inlet velocity value grew.

Effect of blade chord length

As mentioned earlier, the solidity of turbine blades significantly affects wind turbine efficiency. Considering the mathematical equation 17, this parameter depends on the values of chord length and the number of blades. In this section, the effect of changing the values of blade chord length on power and torque coefficients and its impact on the efficiency and output power of the turbine is investigated. The chord length is changed from 0.1(m) to 0.25(m); consequently, the solidity value increases from 1.9 to 4.8. Other relevant and effective parameters such as tip speed ratio and inlet wind speed, are assumed to be constant. The results obtained for the power and torque coefficients values in different TSRs concerning chord length changes are shown in Figs. 8 and 9.

As it is clear from the results, the amount of power and torque coefficients have increased remarkably with increasing the length of the chord. The maximum values of C_p and C_m again are obtained at TSR = 1.8, and their values are calculated to be around 0.462 and 0.098, respectively corresponding to the chord length of 0.25(m), which was 273% higher than C_p value of c =0.1(m). Also, this analysis applies to small-sized turbines with low TSRs (less than 4), and in this case, wind flow involved with a larger cross-section of the turbine blades, which has resulted in higher wind turbine efficiency. Also, with increasing chord length and increasing C_p and C_m values in small TSRs, it is determined that with increasing chord length, the amount of initial torque for self-starting decreases, which in turn improves the optimal design of a vertical axis wind turbine. To illustrate flow behavior around Gorlov VAWT contour plots are given in Fig.10.

Regarding Fig.10, low-velocity area and wake flow regime between blades decreased significantly in the turbine with higher blade chord length; however, wake flow in the downstream section and around the turbine is

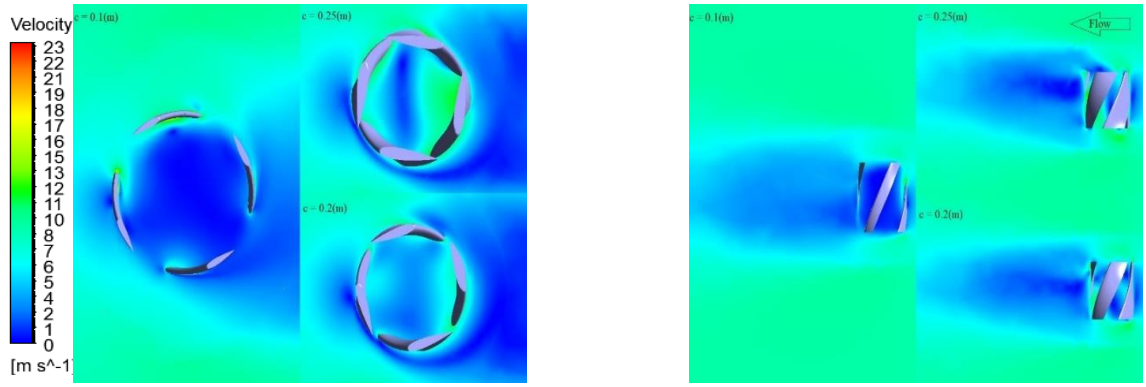

Fig.10: Velocity contour plots for different chord length values

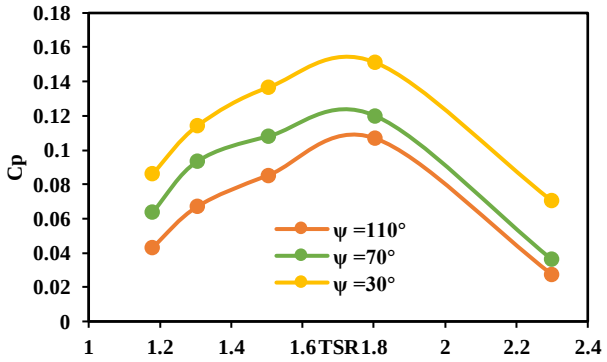

Fig.11: C_p Values at different helical angles

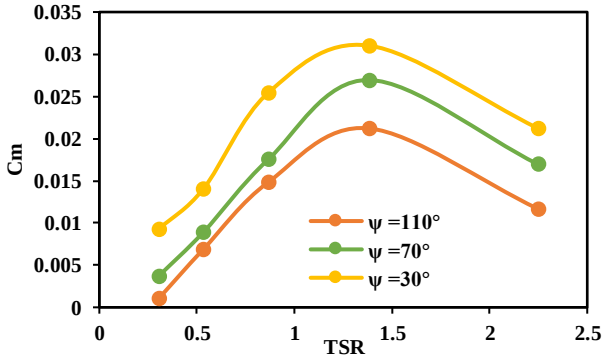

Fig.12: C_m Values at different helical angles

more intensive in configuration with c=0.1. Additionally, the turbine's high-speed area near blade walls was more substantial, with c=0.25(m). Taken together, favorable flow distribution between blades in the rotor with higher chord length was more visible.

Effect of helical angle

In this section, the helical angle of the Gorlov vertical axis wind turbine blades was changed to investigate its effect on the power and torque coefficients, and a suitable helical angle was provided for the design of the four-bladed Gorlov wind turbine. All values related to boundary conditions and geometric detail except the helical angle are considered constant. To analyze the effect of blade helical angle on the performance of the vertical axis wind turbine in this phase of numerical simulation, two helical angles of 30 and 110 degrees were examined next to the initial state. The results of the numerical solution for C_p and C_m at each helical angle are shown in Figs. 11 and 12.

The numerical simulation results, shown in Figs. 9 and 10, show that the maximum C_p and C_m were related to the helical angle of 30 degrees, which is equivalent to 0.151 and 0.031, respectively; which was 30% higher than C_p value of ψ =70(deg). Therefore, it can be claimed that the optimal helical angle in the existing operating conditions for the Gorlov turbine was the helical angle of 30 degrees. With the increase of this design parameter, the efficiency of the mentioned turbine has decreased. On the other hand, due to the more favorable values of C_p and C_m in low TSR in the case where the helix angle had its minimum value, it is assumed that the initial torque for self-starting was less than the other two modes. To illustrate flow behavior around Gorlov VAWT contour plots are given in Fig.13.

Based on Fig.13, lower wake flow is obtained by the higher helical angle between the blades. However, the turbine with ψ =30 (deg) has the ability to produce more power due to its geometric proximity to a turbine

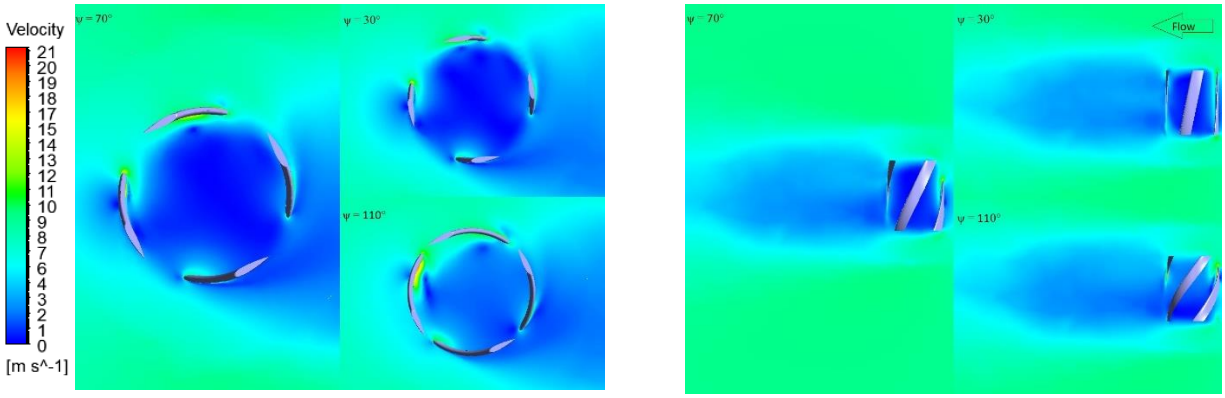

Fig.13: Velocity contour plots for different helical angle values

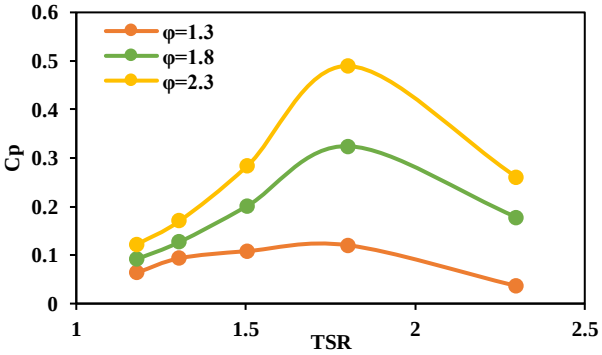

Fig.14: C_p Values at different aspect ratios

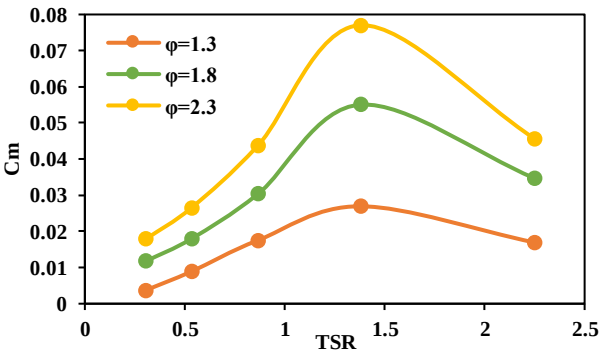

Fig.15: C_m Values at different aspect ratios

with straight blades. It is also essential to consider the limitation of high helical angle turbine construction and operation condition.

Effect of aspect ratio

In this section, the aspect ratio parameter has been studied, the value of which has been calculated from the mathematical relation 16. Changing this parameter has required changes in the height and radius of the turbine. However, it is necessary to assume the turbine's swept area to be constant to calculate different aspect ratios. According to this assumption, the appropriate radius and height values were calculated for the new aspect ratios. In this study, the initial aspect ratio value, according to the geometric information in Table 1, is equal to 1.3. Subsequently, the values of 1.8 and 2.3 were considered according to the mentioned assumption to evaluate the effects of the aspect ratio on the turbine efficiency. For numerical analysis and simulation, fixed TSR values are considered, so according to the new radius, the values of angular velocity (rad/s) and the number of rotations (rpm) change. It should be noted that the radius and height obtained for φ = 1.8 are equal to 0.188(m) and 0.644(m), and for φ = 2.3 are equal to 0.158(m) and 0.728(m), while other geometric parameters, as well as boundary conditions, remain unchanged. The results obtained for C_p and C_m in each aspect ratio were shown in Figs. 14 and 15.

The results from numerical simulations showed that the power and torque coefficients increased significantly with the aspect ratio. The highest values of C_p and C_m were related to φ = 2.3, which were 0.483 and 0.076, respectively, which was 250% higher than C_p value of φ= 1.3. Also, in TSR = 1.8, maximum values for power and torque coefficients have occurred. Therefore, as a result, the turbine will have better performance with the increasing aspect ratio. Considering the increase of these two crucial coefficients in low TSRs, it can be concluded that the turbine needs less initial torque to start. The increase in efficiency and performance improvement in the Gorlov turbine is due to the increase in aspect ratio in small TSRs (less than 4) and small samples. As a result, efficiency increases due to aspect ratio may not occur in large-scale turbines operating at high speeds. To illustrate flow behavior around Gorlov VAWT contour plots are given in Fig.16.

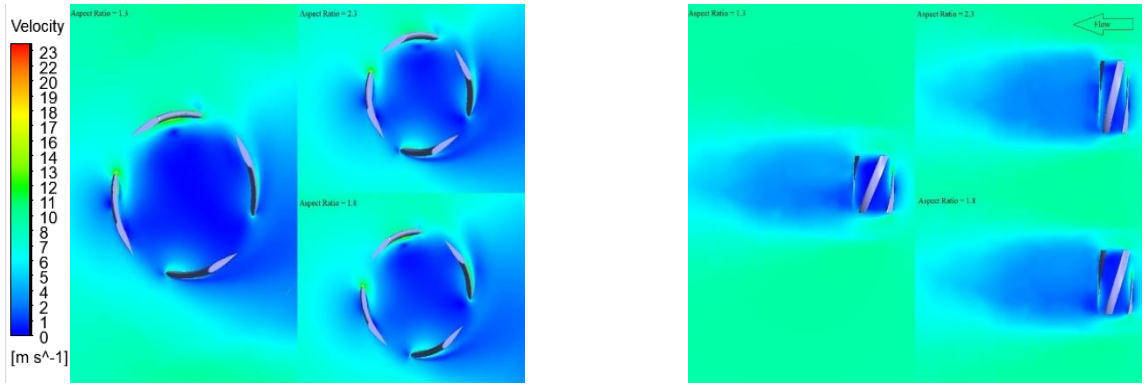

Fig.16 Velocity contour plots for different aspect ratio values

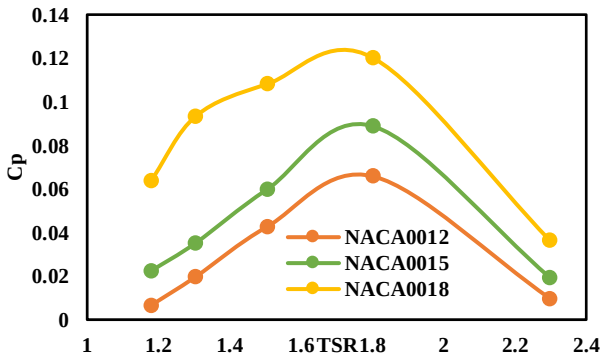

Fig.17: C_p Values at NACA airfoil profiles

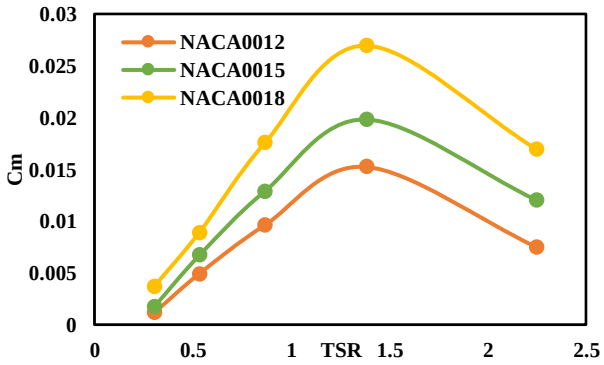

Fig.18: C_m Values at NACA airfoil profiles

As shown in Fig.16, the higher aspect ratio increases the turbine's height, which causes more turbine blade area to be involved with the incoming wind flow, improving turbine performance. However, it causes trapping wake flow between the rotor because of the lower rotor diameter. As the aspect ratio increases, the solidity of the turbine will increase, which will help turbine performance. It should be noted that high aspect ratio turbines have manufacturing considerations and mechanical limitations.

Effect of airfoil profile

The last section investigates the effect of airfoil profiles on the performance and efficiency of the Gorlov turbine. For this purpose, two airfoil profiles, NACA0015 and NACA0012, and NACA0018, which were initially used as blade profiles, were numerically simulated. The results obtained for power and torque coefficients are shown in Figs. 17 and 18.

The results showed that the performance and efficiency of the Gorlov turbine were minimal when the NACA0012 airfoil profile was selected for the design and the values of C_p and C_m were equal to 0.009 and 0.0012, respectively. Due to the small values of C_p and C_m in the initial TSRs, it can be concluded that the mentioned Gorlov turbine with the NACA0012 airfoil profile requires high initial torque for self-starting, which indicates that the NACA0012 airfoil profile should not be chosen for designing. To illustrate flow behavior around Gorlov VAWT contour plots are given in Fig.19.

Based on Fig.19, there is no significant difference in wake flow between the different airfoils. However, the turbine with NACA 0018 profile has a higher thickness which results in the increased power production of the turbine. Furthermore, the wake in the downstream section of the rotor with NACA0012 airfoil profile was slightly more intensive than in other configurations. Also, unfavorable flow separation, which affects turbine performance at the leading edge of the blade, was more significant than rotor with the NACA0018 and NACA0015 airfoil profiles.

OPTIMIZATION

For the optimization process, the experiment needs to be designed first. Since the experiment was pre-designed and the effect of various parameters was investigated, The DOE method was set to the custom mode. Following this,

Table 4: Goodness of fit

Model	Coefficient of Determination	Root Mean Square Error
Kriging	1	5.4758e-9

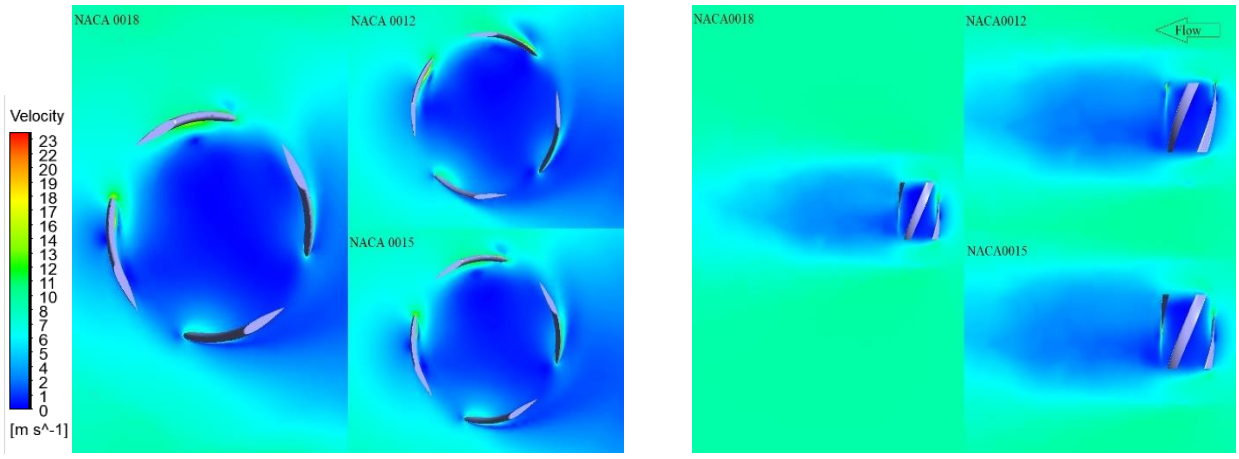

Fig.19: Velocity contour plots for different NACA airfoil profiles

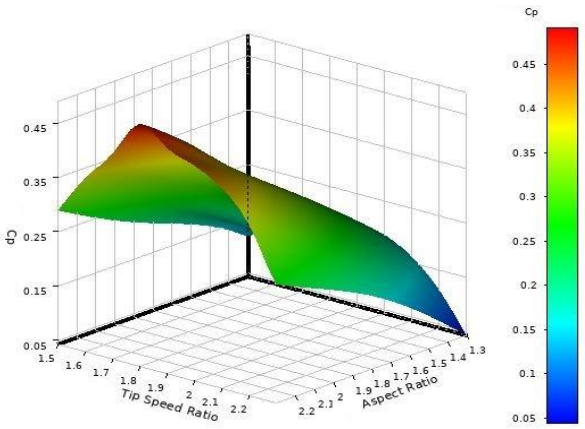

Fig.20: C_P based on TSR and different aspect ratios

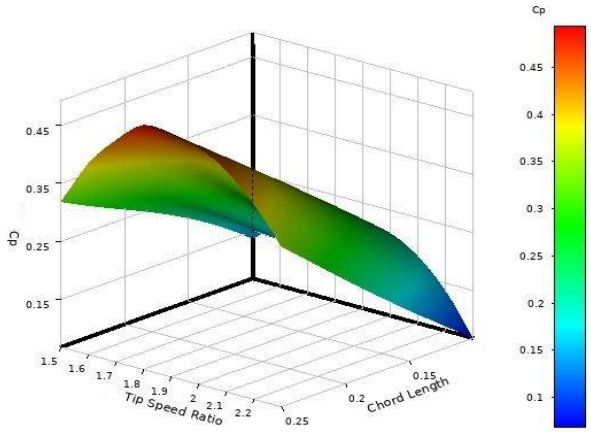

Fig.21: C_P based on TSR and different chord lengths

in the response surface section, different approaches were tried. According to the examination of the existing errors, the Kriging method with variable Kernel variation type was the best and most optimal mode.

All the parameters examined numerically to perform the optimization process are considered. However, since the NACA0018 airfoil profile has had the best performance in any different operating conditions, the impact of the type of airfoil profile has been omitted . Subsequently, various diagrams were obtained based on the Kriging method, which is shown in Figs. 20 to 23.

According to the above diagrams, the best power coefficient was illustrated at about 0.486.

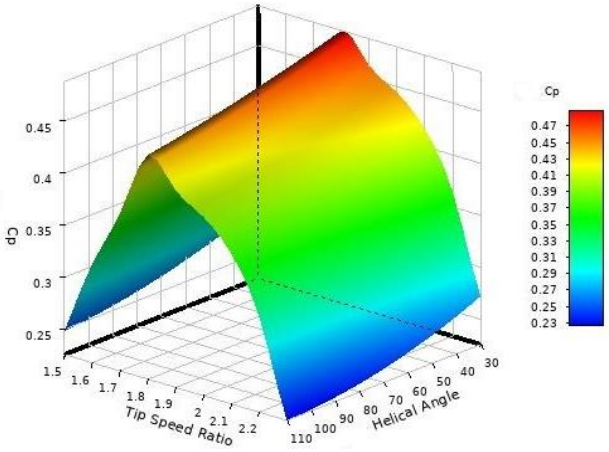

Fig.22: C_P based on TSR and different helical angles

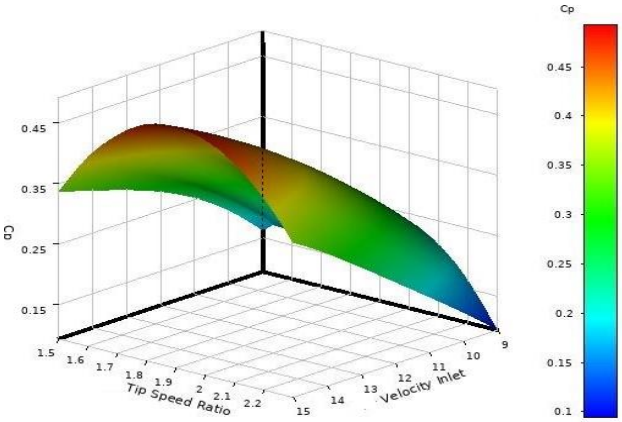

Fig.23: C_p based on TSR and different inlet velocities

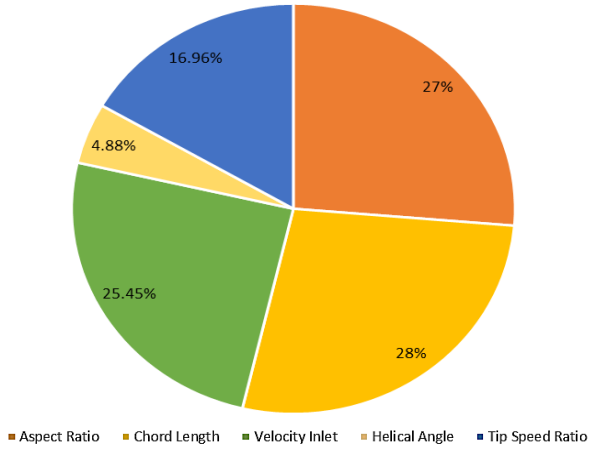

Fig.24: Local sensitivity

The sensitivity coefficient of the parameters was obtained, and that is shown in the below pie chart.

Looking at Fig.24, the chord length has the highest, and the helical angle has the most negligible effect on the power coefficient of the turbine at 28% and 4.88%, respectively. This means that in the examined geometry, the effects of changes in the chord length design parameter values have significantly changed the performance and efficiency of the turbine. On the other hand, changes in the helical angle values have less effect on the results of the turbine efficiency and Cp. As a result, the investigated turbine is sensitive to the chord length and should be given more attention during design.

Finally, the optimal operating conditions were determined after the optimization process with the mentioned method, which are given in Table 5.

The optimal geometry was implemented in SolidWorks designing software. Then it was imported to Ansys Meshing,

Table 5: Operating Conditions of The Optimal Geometry

	Quantity	Value
1	Aspect Ratio	2.2976
2	Chord Length	0.2495 (m)
3	Velocity Inlet	14.9140 (m/s)
4	Helical Angle	31.0690°
5	TSR	1.8907
6	Airfoil Profiles	NACA0018

and the appropriate mesh was created, and then it was simulated in Ansys CFX. After that, the power coefficient was calculated at 0.486, which was 305% higher than the previous configuration.

Also, in order to determine the effect of the varying parameters over the performance of the system and whether they are significant or insignificant, analysis of variance (ANOVA) was also performed. The results of ANOVA are shown in Table 6.

In Table 6, first row is the analyzed parameters namely inlet velocity, blade chord length, helical angle, aspect ratio and blade airfoil profile and cases represent different values of each parameter. Regarding the details of Table 6, as F is larger than F_{crit} and P is smaller than 0.05, the individual parameters and the cases and their interactions are the influential factors on the C_p, and the test is significant. Also as P is much smaller than 0.05, the mathematical results are valid.

CONCLUSIONS

In this study, a numerical solution and simulation based on computational fluid dynamics methods were performed on the design parameters namely inlet wind velocity, blade chord length, helical angle, aspect ratio, and blade airfoil profile of a small-scale Gorlov vertical axis wind turbine using CFX finite volume software. The effect of these sensitive geometric and operational parameters on the performance and efficiency of Gorlov VAWT was done by calculating and studying the two parameters of power and torque coefficient and the diagram of these two dimensionless coefficients in terms of TSR was drawn in the simulation stage. It should be noted that all numerical simulations, mesh independent solutions, and validation of the results were performed with data based on the experimental study, which showed the appropriate accuracy of the simulation. In this article, the use of the Kriging optimization method, which is one of the most reliable optimization

Table 6: ANOVA for simulating the CFD numerical results

Source of variation	SS	df	MS	F	P-value	F_{crit}
Parameters	0.214204	4	0.053551	8.683081	1.35E-05	2.525215
Cases	0.91079	2	0.45539	7.384012	0.001359	3.150411
Interactions	0.153346	8	0.019168	3.10805	0.005302	2.096968
Within	0.370037	60	0.006167	-	-	-
Total	0.828666	74	-	-	-	-

approaches, determined the optimal geometrical and operating conditions based on the obtained CFD results for the prototype, which is an innovative design of the H-rotor VAWT. In addition, the sensitivity of the studied geometry to mentioned design parameters has explained.

The main conclusions and summary of the study are as follows:

- The first operational parameter that was evaluated was the effect of inlet wind speed on the efficiency of the Gorlov wind turbine. For this purpose, the impact of three inlet wind speeds of 9(m/s), 12(m/s), and 15(m/s) on C_p and C_m was investigated. The results showed that by increasing the inlet wind speed, the power and torque coefficients increase significantly, increasing efficiency and improving the turbine's performance. Also, with increasing wind speed, the initial self-starting of the turbine became more proper.
- Another parameter whose effect on the performance of the Gorlov turbine was studied was the chord blade length, which affects the rotor blade's solidity. For this purpose, three different chord lengths of 0.1(m), 0.2(m), and 0.25(m) were examined. The results showed that C_p and C_m increased with increasing chord length, indicating that in small-scale Gorlov turbines, efficiency increases with increasing chord length. Self-start condition also has improved with increasing C_p and C_m. Finally, this performance improvement applies to low TSRs in small-scale turbines operating at low rotations.
- Another design parameter that was evaluated was the Gorlov turbine winding angle. Three different helical angles of 30°,70°, and 110° were examined for this step. The results showed that the turbine's efficiency decreased with increasing helical angles at an angle of 30° degrees, where C_p and C_m values are higher in low TSRs. The initial torque required for self-starting is less.
- Another important parameter that was considered to evaluate the efficiency of wind turbines was the aspect ratio. The radius and height of the rotor were changed according to the constant value of the swept area. Therefore values of 1.3, 1.8, and 2.3 were assumed as aspect ratios. The results showed that in the small-scale Gorlov turbine studied, the C_p and C_m values increased with the rising aspect ratio, and the turbine performance improved. According to the results, the turbine started with less initial torque, and the regular behavior increases C_p and C_m when the turbine is operating at low TSRs.
- The last parameter that was numerically simulated was comparing the performance and efficiency of three different airfoil profiles, NACA0012, NACA0018, and NACA0015. The results showed that the NACA0018 airfoil has the highest efficiency.
- In the reference article [25], the highest power coefficient was evaluated at 0.116; in this section was an attempt to optimize it and obtain a higher power coefficient. Due to the change of various parameters and the optimization process, the best possible geometry was obtained. Its power coefficient was equal to 0.486. This value was calculated due to a numerical simulation, and the Also as all of the numerical and CFD simulations, which are based on the U-RANS equations, there is some lack of predictions specially in low Reynolds number flow regimes and that is suggested to study the aerodynamic performance of Gorlov turbine with more complicated and accurate approaches like LES method or experimentally in a low-speed wind tunnel. In addition, to enhance the self-starting capability of this lift-based turbine, it can be coupled with Savonius drag-based turbine in further studies.

Nomenclature

Symbols

V	Inlet flow velocity (m/s)
N	Number of rotation (rpm)
M	Torque (N.m)
P	Output power (W)
R	Rotor radius (m)
H	Rotor height (m)
A	Swept Area (m^2)
C_p	Power coefficient
C_m	Torque coefficient
c	Blade chord (m)
n	Number of blades

Greek

μ	Viscosity (Pa.s)
ψ	Helical angle
ω	Angular velocity (rad/s)
ρ	Density (kg/m^3)
φ	Aspect ratio
σ	Solidity

Subscript

t	Turbulence
w	Wind flow

Abbreviations

VAWT	Vertical axis wind turbine
HAWT	Horizontal axis wind turbine
CFD	Computational fluid dynamic
DMST	Double multi-stream tube
URANS	Unsteady Reynolds averaged Naive Stokes
TSR	Tip speed ratio

Received : Sep. 11, 2022 ; Accepted : Nov. 21, 2022

REFERENCES

[1] Dixon S. L., Hall C. A., "Fluid Mechanics and Thermodynamics of Turbomachinery", 7th Edition. Amsterdam ; Boston: Butterworth-Heinemann is an Imprint of Elsevier (2014).

[2] Maleki A., Pourfayaz F., Optimal Sizing of Autonomous Hybrid Photovoltaic/Wind/battery Power System with LPSP Technology by Using Evolutionary Algorithms, *Solar Energy*., **115**: 471–483 (2015).

[3] Sleiti A. K., Tidal Power Technology Review with Potential Applications in Gulf Stream, *Renewable and Sustainable Energy Reviews*, **69**: 435–441 (2017).

[4] Maleki A., Hafeznia H., Rosen M. A., Pourfayaz F., Optimization of a Grid-Connected Hybrid Solar-Wind-Hydrogen CHP System for Residential Applications by Efficient Metaheuristic Approaches, *Applied Thermal Engineering*, **123**: 1263–1277 (2017).

[5] M. Khudri Johari, Azim M., Jalil A., Faizal Mohd Shariff M., Comparison of Horizontal Axis Wind Turbine (HAWT) and Vertical Axis Wind Turbine (VAWT), *IJET*, **7(4.13)**: 74 (2018).

[6] A. G. Abo-Khalil et al., "Design of State Feedback Current Controller for Fast Synchronization of DFIG in Wind Power Generation Systems," *Energies*, 1**2 (12):** 2427 (2019).

[7] Eriksson S., Bernhoff H., Leijon M., "Evaluation of Different Turbine Concepts for Wind Power," *Renewable and Sustainable Energy Reviews*, **12(5)**: 1419–1434 2008).

[8] Bansal R.C., Bhatti T.S., Kothari D.P., On Some of the Design Aspects of Wind Energy Conversion Systems, *Energy Conversion and Management*, **43(16)**: 2175–2187 (2002).

[9] Hand B., A review on the Historical Development of the Lift-Type Vertical Axis Wind Turbine_ From Onshore to Offshore Floating Application, *Sustainable Energy Technologies and Assessments*, **11**: (2020).

[10] Maldonado R.D. et al., Design, Simulation and Construction of a Savonius Wind Rotor for Subsidized Houses in Mexico, *Energy Procedia*, **57**: 691–697 (2014).

[11] Burton T., Ed., "Wind Energy: Handbook". Chichester, New York: J. Wiley, (2001).

[12] Aslam Bhutta M.M., Hayat N., Farooq A.U., Ali Z., Jamil Sh. R., Hussain Z., Vertical Axis Wind Turbine – A Review of Various Configurations and Design Techniques, *Renewable and Sustainable Energy Reviews*, **16(4)**: 1926–1939 (2012).

[13] Akhlaghi M., Ghafoorian F., The investigation of Arc Angle Rotor Blade Variations Effect of the Savonius Vertical Axis Wind Turbine on the Power and Torque Coefficients, Using 3D Modeling, *Renewable Energy Research and Applications*, (2022).
[14] Pallotta A., Pietrogiacomi D., Romano G.P., HYBRI – A combined Savonius-Darrieus wind TURbine: Performances and Flow Fields, *Energy*, **191**: 116433 (2020).
[15] Borzuei D., Moosavian S.F., Farajollahi M., On the Performance Enhancement of the Three-Blade Savonius Wind Turbine Implementing Opening Valve, *Journal of Energy Resources Technology*, 11.
[16] Winchester J., Torque Ripple and Variable Blade Force: A Comparison of Darrieus and Gorlov-Type Turbines for Tidal Stream Energy Conversion, 9.
[17] Moghimi M., Developed DMST Model for Performance Analysis and Parametric Evaluation of Gorlov Vertical Axis Wind Turbines, *Sustainable Energy Technologies and Assessments*, 15 (2020).
[18] Chong W.-T., et al., Cross Axis Wind Turbine: Pushing the Limit of Wind Turbine Technology with Complementary Design, *Applied Energy*, **207**: 78–95 (2017).
[19] Jayaram V., Bavanish B., A Brief Review on the Gorlov Helical Turbine and its Possible Impact on Power Generation in India, *Materials Today: Proceedings*, **37**: 3343–3351(2021).
[20] Wardhana W., Keniraras N., Pratama R. S., Rahmawati S., "Hydrodynamics Performance Analysis of Vertical Axis Water Turbine (VAWT) Gorlov Type Using Computational Fluid Dynamics (CFD) Approach", *IOP Conf. Ser.: Earth Environ. Sci.*, **698(1)**: 012022 (2021).
[21] Jayaram V., Bavanish B., Design and Analysis of Gorlov Helical Hydro Turbine on Index of Revolution, *International Journal of Hydrogen Energy*, 47(77) 32804–32821 (2022).
[22] Chen J., Yang H.X., C. P. Liu, C. H. Lau, and M. Lo, A novel vertical axis water turbine for power generation from water pipelines, *Energy*, **54**:184–193, (2013).
[23] Bachant P., Wosnik M., Performance Measurements of Cylindrical- and Spherical-Helical Cross-Flow Marine Hydrokinetic Turbines, with Estimates of Exergy Efficiency, *Renewable Energy*, **74**: 318–325 (2015).
[24] Alaimo A., Esposito A., Messineo A., Orlando C., Tumino D., 3D CFD Analysis of a Vertical Axis Wind Turbine, *Energies*, **8 (4)**:3013–3033 (2015).
[25] Cheng Q., Liu X., Ji H.S., Kim K.C., Yang B., Aerodynamic Analysis of a Helical Vertical Axis Wind Turbine, *Energies*, **10(4)**: 575 (2017).
[26] Krishnaraj J., Additive Manufacturing of a Gorlov Helical Type Vertical Axis Wind Turbine, *IJEAT*, **9(2)**: 2639–2644 (2019)
[27] Rabei, Ivan, experimental Observations on Efficiency Difference Between Helical and Straight Bladed Vertical Axis Wind Turbines, (2020).
[28] Howell R., Qin N., Edwards J., Durrani N., Wind Tunnel and Numerical Study of a Small Vertical Axis Wind turbine, *Renewable Energy*, **35(2)**: 412–422, (2010).
[29] Siddiqui M.S., Rasheed A., Kvamsdal T., Tabib M., Effect of Turbulence Intensity on the Performance of an Offshore Vertical Axis Wind Turbine, *Energy Procedia*, **80**: 312–320 (2015).
[30] Hosseinkhani A., Sanaye S., Performance Prediction of a SANDIA 17-m Vertical Axis Wind Turbine Using Improved Double Multiple Streamtube, **14(12)**: 5 (2020).
[31] Moghimi M., Motawej H., Investigation of Effective Parameters on Gorlov Vertical Axis Wind Turbine, *Fluid Dyn*, **55(3)**: 345–363 (2020)
[32] Carbó Molina A., De Troyer T., Massai T., Vergaerde A., Runacres M.C., Bartoli G., Effect of Turbulence on the Performance of VAWTs: An Experimental Study in Two Different Wind Tunnels, *Journal of Wind Engineering and Industrial Aerodynamics*, **193**:103969 (2019).
[33] Chatelain P., et al., Investigation of the Effect of Inflow Turbulence on Vertical Axis Wind Turbine Wakes, *J. Phys.: Conf. Ser.*, 854 012011 (2017).
[34] Rezaeiha A., Montazeri H., Blocken B., On the Accuracy of Turbulence Models for CFD Simulations of Vertical Axis Wind Turbines, *Energy*, 180: 838–857 (2019).
[35] Nichols R.H., Turbulence Models and Their Application to Complex Flows, 214 (2010).
[36] Adaramola M.S., Krogstad P.-Å., Experimental Investigation of Wake Effects on Wind Turbine Performance, *Renewable Energy*, **36(8)**: 2078–2086 (2011)

[37] Sahebzadeh S., Rezaeiha A., Montazeri H., Vertical-Axis Wind-Turbine Farm Design: Impact of Rotor Setting and Relative Arrangement on Aerodynamic Performance of Double Rotor Arrays," *Energy Reports*, **8**: 5793–5819 (2022).

[38] Danao L.A., Eboibi O., Howell R., An Experimental Investigation Into the Influence of Unsteady Wind on the Performance of a Vertical Axis Wind Turbine, *Applied Energy*, **107**: 403–411 (2013)

[39] Li Z., et al., Three-Dimensional Simulation of Wind Tunnel Diffuser to Study the Effects of Different Divergence Angles on Speed Uniform Distribution, Pressure in Outlet, and Eddy Flows Formation in the Corners, *Physics of Fluids*, 17(2020).

[40] Silva-Llanca L., Inostroza-Lagos S., Optimum Power Generation Assessment in an H-Darrieus Vertical Axis Wind Turbine *via* Exergy Destruction Minimization, *Energy Conversion and Management*, **243**: 114312, (2021).

[41] Tahani M., et al., Investigating the Effect of Geometrical Parameters of an Optimized Wind Turbine Blade in Turbulent Flow, *Energy Conversion and Management*, **153**: 71–82 (2017).

[42] *Jayaram V., Bavanish B.*, A Brief Study on the Influence of the Index of Revolution on the Performance of Gorlov Helical Turbine, *IJRER*, **12(2)**: (2022).

[43] Delafin P., Nishino T., Wang L., Kolios A., Effect of the Number of Blades and Solidity on the Performance of a Vertical Axis Wind Turbine, *J. Phys.: Conf. Ser.*, **753**: 022033 (2016).

[44] Brusca S., Lanzafame R., Messina M., Design of a Vertical-Axis Wind Turbine: How the Aspect Ratio Affects the turbine's performance, *Int J Energy Environ Eng*, **5(4)**: 333–340 (2014).

[45] Fouest S.Le., Mulleners K., The Dynamic Stall Dilemma for Vertical-Axis Wind Turbines, *Renewable Energy*, **198**: 505–520 (2022).

[46] ArabGolarche A., Moghiman M., Javadi MalAbad S.M., Investigation of Effective Parameters on Darrieus Wind Turbine Efficiency with Aerodynamics Models, (2015).

[47] Mohamed O.S., Ibrahim A.A., Etman A.K., Abdelfatah A.A., Elbaz A.M.R., Numerical Investigation of Darrieus Wind Turbine with Slotted Airfoil Blades, *Energy Conversion and Management: X*, **5**: 100026 (2020).

[48] Ismail M.F., Vijayaraghavan K., The Effects of Aerofoil Profile Modification on a Vertical Axis Wind Turbine Performance, *Energy*, **80**: 20–31 (2015).

[49] Li Q., Maeda T., Kamada Y., Murata J., Furukawa K., Yamamoto M., Effect of Number of Blades on Aerodynamic Forces on a Straight-Bladed Vertical Axis Wind Turbine, *Energy*, **90**: 784–795 (2015).

[50] Jafari M., Razavi A., Mirhosseini M., Effect of Airfoil Profile on Aerodynamic Performance and Economic Assessment of H-Rotor Vertical Axis Wind Turbines, *Energy*, **165**: 792–810 (2018).

[51] Donisi L., et al., Airfoil Catalogue for Wind Turbine Blades with Openfoam, 18.

[52] Divakaran U., Ramesh A., Mohammad A., Velamati R.K., "Effect of Helix Angle on the Performance of Helical Vertical Axis Wind Turbine, *Energies*, **14(2)**: 393 (2021).

[53] Bedon G., Raciti Castelli M., Benini E., Optimization of a Darrieus Vertical-Axis Wind Turbine Using Blade Element – Momentum Theory and Evolutionary Algorithm, *Renewable Energy*, **59**: 184–192 (2013).

[54] Yang B., Shu X.W., Hydrofoil Optimization and Experimental Validation in Helical Vertical Axis Turbine for Power Generation from Marine Current, *Ocean Engineering*, 42: 35–46 (2012).

[55] Noman A.A., Tasneem Z., Sahed Md.F., Muyeen S.M., Das S.K., F. Alam, Towards Next Generation Savonius Wind Turbine: Artificial Intelligence in Blade Design Trends and Framework, *Renewable and Sustainable Energy Reviews*, **168**: 112531 (2022).

[56] Chen W.-H., Wang J.-S., Chang M.-H., Mutuku J.K., Hoang A.T., Efficiency Improvement of a Vertical-Axis Wind Turbine Using a Deflector Optimized by Taguchi Approach with Modified Additive Method, *Energy Conversion and Management*, **245**: 114609 (2021).

[57] Zhang B., Song B., Mao Z., Tian W., A Novel Wake Energy Reuse Method to Optimize the Layout for Savonius-Type Vertical Axis Wind Turbines, *Energy*, **121**: 341–355 (2017).

[58] Ranjbar M.H. et al., Power Enhancement of a Vertical Axis Wind Turbine Equipped with an Improved Duct, *Energies*, **14(18)**: 5780 (2021).

[59] Bourguet R., Martinat G., Harran G., Braza M., Aerodynamic Multi-Criteria Shape Optimization of VAWT Blade Profile by Viscous Approach, in "Wind Energy", Heidelberg: Springer Berlin Heidelberg, 215–219 (2007).

[60] Said M.S.M., Ghani J A., Kassim M.S., Tomadi S.H., Haron C., Comparison Between Taguchi Method and Response Surface Methodology (RSM) in Optimizing Machining Condition, 60–68 (2013).

[61]Sudasna-Na-Ayudthya P., Comparison of Response Surface Model and Taguchi Methodology for Robust Design, 157.

[62] Stergiannis N., Lacor C., Beeck J.V., Donnelly R., CFD Modelling Approaches Against Single Wind Turbine Wake Measurements Using RANS, *J. Phys.: Conf. Ser.*, **753**: 032062 (2016).

[63] Liamis N., Lebert Y., "Implementation of a Low Reynolds k-Epsilon Turbulence Model in a 3D Navier-Stokes Solver for Turbomachinery Flows", 3*1st Joint Propulsion Conference and Exhibit*, San Diego,CA, USA, (1995).

[64]Mao Z.,Tian W., Effect of the Blade Arc Angle on the Performance of a Savonius Wind Turbine, *Advances in Mechanical Engineering*, **7(5)**: 168781401558424 (2015).